

Effect of humidity and temperature on nano/microtribological properties of perfluorinated carboxylic acid and hydrogenated carboxylic acid self-assembled monolayers deposited on aluminum-coated silicon substrate

Yufei Mo^{a,b} and Mingwu Bai^{a*}

Two series of perfluorinated carboxylic acid (FC) and hydrogenated carboxylic acid (HC) self-assembled monolayer (SAM) films were prepared on aluminum surfaces separately by chemical vapor deposition. The formation, structure and morphology of these films were characterized by measuring contact angle with ellipsometric method, x-ray photoelectron spectrometry, and atomic force microscopy, respectively. FC and HC SAMs with long chains formed more densely packed films than those with short chains did. The comparative micro/nanoscale friction and adhesive properties of FC and HC SAMs, with various chain lengths on aluminum-coated silicon substrate, were investigated. The influence of environmental conditions, such as relative humidity (RH) and temperature, on the friction and adhesion behavior was studied. Micro/nanotribological properties of the films were greatly influenced by their backbones and terminal groups. FC SAMs with long chain exhibited adhesion-resistance, friction reduction, and environmental independence. Copyright © 2009 John Wiley & Sons, Ltd.

Keywords: SAM; perfluorinated carboxylic acids; hydrogenated carboxylic acids; nanotribology; microtribology

Introduction

Micro/nanoelectromechanical systems (MEMS/NEMS) have developed rapidly in the past decades because of their superior performance and low unit cost.^[1] However, large surface area-to-volume ratio causes serious adhesive and frictional problems for MEMS operations.^[2] Recently, aluminum-coated substrates have gained importance, particularly after the commercial application of digital micromirror devices (DMD) and micro/nanooptoelectromechanical system (MOEMS/NOMES) devices.^[3] The reliability of these devices necessitates the use of molecularly thin lubricants for wear protection. Self-assembled monolayers (SAMs) have been widely investigated over the past years because of their potential applications in the fields of surface modification, boundary lubricants, sensors, photoelectronics, wetting and functional biological interaction.^[4–11] On the basis of the surface chemical reaction and synthetic approach, the chemical structures of SAMs can be manipulated easily at both individual molecular and material levels.^[12–15] As ideal molecular lubricants for MEMS, SAMs have been given great attention to solve the friction related problems.^[16] Alkylthiols, alkylsilanes and alkylphosphonates which are produced on gold and silicon surfaces are the main popular systems to be used for this purpose.^[17–23] However, so far only few researchers have reported the tribological behavior of perfluorinated carboxylic acid (FC) and hydrogenated carboxylic acid (HC) SAMs on aluminum-coated substrate, which is critical for their application in MEMS/NEMS. SAMs consist of a head group, backbone group and terminal group.^[4,24] The appropriate choice

of the three kinds of groups will contribute to optimal design of the SAMs. Deposition of SAMs uses either liquid phase or vapor phase deposition. Liquid phase deposition is a convenient, fast, and universal process. On the other hand, vapor phase deposition requires a special reactor. However, it overcomes the limitations of liquid phase deposition, such as difficulty in dissolving the reactants and incomplete coverage of surfaces.

In this work, a comparative research is presented on the surface and micro/nanotribological properties of FC and HC SAMs on aluminum-coated silicon substrate formed by chemical vapor deposition (CVD). Furthermore, the influence of environmental conditions, such as relative humidity (RH) and temperature, on tribological performance of these SAMs, was investigated. In addition, the corresponding tribological mechanism on molecular scale was discussed. This study is expected to provide a valuable guide in design and selection of appropriate SAMs for lubrication and protection of MOEMS/NOEMS.

* Correspondence to: Mingwu Bai, State Key Laboratory of Solid Lubrication, Lanzhou Institute of Chemical Physics, Chinese Academy of Sciences, Lanzhou 730000, China. E-mail: nanolab@lzb.ac.cn

a State Key Laboratory of Solid Lubrication, Lanzhou Institute of Chemical Physics, Chinese Academy of Sciences, Lanzhou 730000, China

b Graduate School of Chinese Academy of Sciences, Beijing 100039, China

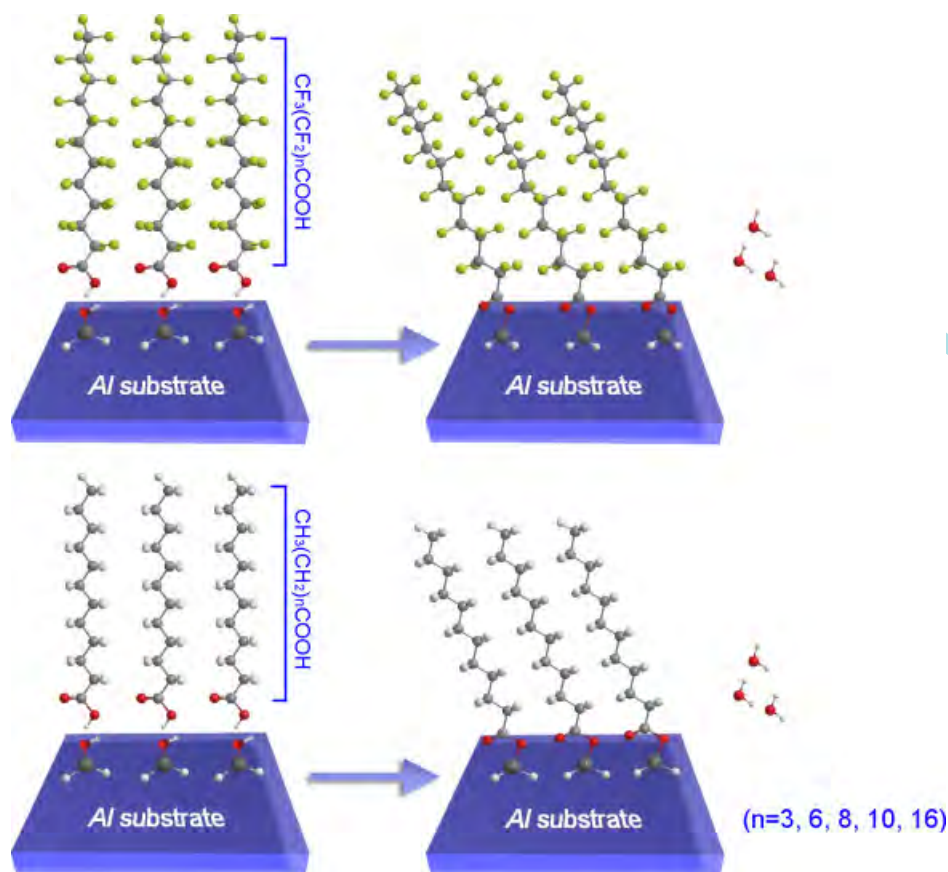


Figure 1. Schematic structure and forming process of perfluorinated carboxylic acid and hydrogenated carboxylic acid molecules adsorbed chemically onto Al substrate. This figure is available in colour online at www.interscience.wiley.com/journal/sia.

Experimental

Materials and deposition technique

The thin aluminum coating of 100 nm thickness was produced by sputter-coating at room temperature under high vacuum. Pieces of commercial silicon wafer, P-type 100, with each size of approximately $20 \times 10 \times 0.5$ mm, were used as substrates for SAMs deposition. A homologous series of chain length perfluorinated carboxylic acid (FC; 97%, $\text{CF}_3(\text{CF}_2)_n\text{COOH}$, $n = 3, 6, 8, 10, 16$, viz C5-C18) were purchased from ABCR GmbH & Co. KG, and hydrogenated carboxylic acid (HC; 97%, $\text{CH}_3(\text{CH}_2)_n\text{COOH}$, $n = 3, 6, 8, 10, 16$, viz C5-C18) were obtained from Hushi Chemical Co., Ltd. Shanghai and were used as received.

In our present research, two kinds of SAMs, namely FC and HC, were formed on the aluminum-coated silicon substrate by CVD. The procedure is detailed as follows. The samples were placed in a 100-ml sealed vessel with a glass container filled with 0.2 ml FC or HC precursor. There was no direct contact between the samples and precursor. The vessel was placed in an oven and then nitrogen gas was filled in the oven. The samples were annealed in nitrogen at 200°C for 3 h, and then cooled in a desiccator. The precursor vaporized and reacted with substrate surface on each sample, resulting in the formation of SAM. Then, the samples were rinsed with chloroform, acetone, ethanol, and deionised water successively to remove other physisorbed ions and molecules. The deposition of SAMs relied on the chemisorption of reactive head groups presented in the adsorbate molecules on the substrate surface in order to anchor them. The aluminum surface was

converted into aluminum oxide under ambient conditions and adsorbed water caused hydroxylation of the oxide layer.^[25] Fig. 1 shows the mechanism of adsorption of SAMs. FC and HC SAMs are of similar chain length and head group monolayers with different backbone groups.

Characterization of the films

The static contact angles for ultra-pure water on the films were measured with a CA-A type contact angle meter (Kyowa Scientific Co. Ltd.). At least five replicate measurements were carried out for each specimen and the measurement error was $\pm 1^\circ$.

The film thickness was measured on a L116-E ellipsometer (Gaertner, USA), which was equipped with a He-Ne laser (632.8 nm) set at an incident angle of 50° . A real refractive index of 1.45 was set for the aluminum oxide layer and 1.38 for organic layers. The data were collected from 10 different positions for each specimen to get the averaged value.

Chemical composition and structure of the surface were examined with a PHI-5702 multi-technique X-ray photoelectron spectrometer (XPS), using a pass energy of 29.35 eV, an excitation source of Mg-K α radiation ($h\nu = 1253.6$ eV) and take-off angle of 36° . The chamber pressure was about 3×10^{-8} torr during operation. Peak deconvolution and quantification of elements were accomplished using the software and sensitivity factors supplied by the manufacturer. The binding energy of adventitious carbon (C_{1s} ; 284.8 eV) was used as a reference.

The nanotribological behavior of the two kinds of films was characterized with an atomic force microscope/friction force microscope (AFM/FFM) controlled by CSPM4000 electronics, using the contact mode. Commercially available rectangle Si_3N_4 cantilevers with a normal force constant, 0.4 N/m, a radius of less than 25 nm and backside coated by gold (Budgetsensors Instruments Inc.) were employed. The force distance curves were recorded and the pull-off force was reckoned as the adhesive force, which was given by $F = K_c Z_p$. K_c is force constant of the cantilever and Z_p is vertical displacement of the piezotube, that is, the deflection of the cantilever.^[26,27]

The friction force is a lateral force exerted on a tip during scanning and can be measured using the twist of the tip/cantilever assembly. To obtain friction data, the tip was scanned back and forth in the x-direction in contact with sample at a constant load while the lateral deflection of the lever was measured. The differences in the lateral deflection or friction signal between back and forth motions were proportional to the friction force. The friction force was calibrated by the method described in Ref. [28]. Friction forces were continuously measured with various external loads. The load was increased or decreased linearly in each successive scan line and typically normal loads ranged from 5 to 100 nN. Scanning for the measurement of friction force was performed at a rate of 1 Hz along the scan axis and with a scan size of $1 \mu\text{m} \times 1 \mu\text{m}$ (viz. sliding velocity of $2 \mu\text{m/s}$). The scan axis was perpendicular to the longitudinal direction of the cantilever. The sets of data were displayed graphically in a friction image.

The influence of RH and temperature on adhesion was studied in a noise and vibration-isolated and environment controlled booth, as shown in Fig. 2. RH was controlled by introducing a mixed stream of dry and moist nitrogen into the booth, while the temperature was maintained at $20 \pm 2^\circ\text{C}$. In order to study the effect of temperature on adhesion, an optical heater was employed to minimize thermal effect on AFM cantilever and PbZrTiO₃ (PZT) scanner. A thermocouple and a hygrometer were used to measure temperature and RH, respectively of the sample. The temperature ranged from 20 to 90°C , while the RH was maintained at $45 \pm 5\%$ RH during adhesion measurement.

The microtribological behavior of films was characterized with a novel ball-on-inclined plane microtribotester. It was first developed at National Institute of Standards and Technology (NIST) during the year 2000,^[29–31] and in the present work moving stage with nanometer resolution and inclined plane with resolution of 0.035° were used. A standard AISI-52 100 steel ball of 3.18 mm in diameter was selected as the counterpart. The root-mean-square (RMS) roughness of the ball was estimated to be about 24 nm, by using AFM. After ultrasonicing in acetone, the ball was fixed in a stationary holder sustained by a beam and the samples were then mounted on the moving stage. The main idea of the test is to measure the shear rupture strength and durability of several nanometers of films on surfaces of nanometer scale roughness. Briefly, the ball slides along or multi impacts the sample on an inclined plane. The load is controlled by the geometric interference of the two surfaces and the forces in the three dimensions are continuously recorded by a force transducer mounted on top of the ball. The angle of incline of the flat plane controls the initial loading and the rate of load increase. The large area of contact between the ball and the flat surfaces captures a large number of molecules and upon deformation of the surfaces as the load increases, the contact area increases. At a load where the film can not sustain the shear stresses, the film ruptures. The abrupt increase of friction coefficient indicates the failure of film under

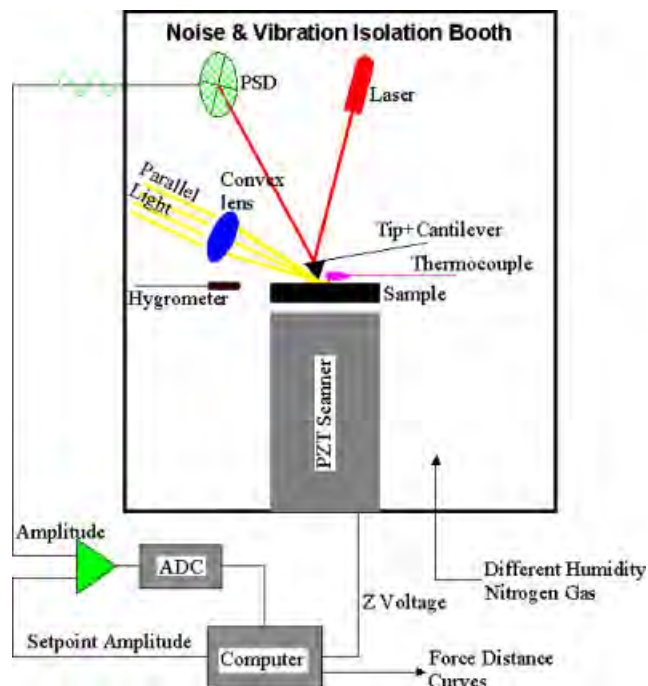


Figure 2. A schematic figure of AFM system used for adhesion measurement. This figure is available in colour online at www.interscience.wiley.com/journal/sia.

the test condition of applied load and impact cycles. To avoid the effect of dust particles, all measurements were done in a class-10 clean room at a RH of 15% and temperature of 20°C .

Results and Discussion

Structure and surface characterization

Measurement of static contact angle is an effective way to reflect the variation of chemical composition on the surface. The contact angles for water on Al surface and the SAMs are shown in Fig. 3. FC and HC SAMs exhibited larger contact angles than aluminum surface. Furthermore, the FC SAMs showed higher contact angles than HC SAMs, as a result of the $-\text{CF}_3$ terminal groups with lower surface energy in comparison with $-\text{CH}_3$ terminal groups.^[32] The thickness values of FC and HC SAMs are listed in Table 1. The variation of contact angle and thickness indicates that two series of molecules have successfully adsorbed chemically on Al surface. Figure 1 shows the chemical structures for the two series of SAMs produced for this study.

In order to obtain information on the surface characteristics, such as uniformity, roughness, and distribution, the surface morphology of prepared films was measured using AFM. The typical AFM morphologies of bare Al, FC12 and HC12 surfaces are shown in Fig. 4a, b, c, respectively. It is shown that the films are regularly distributed on the Al surface and the surfaces of the films are rather smooth at micrometer scale with a RMS roughness of about 0.78 nm. FC film has a RMS roughness of about 0.43 and 0.52 nm for HC film over a scan size of $1 \mu\text{m} \times 1 \mu\text{m}$.

X-ray photoelectron spectroscopy (XPS) was used to evaluate the relative atomic composition on the surface of SAMs. The procedure involved the measurement of the Al2p, F1s and C1s core level spectra for surfaces of these films. The data of Al2p features from bare aluminum surface are shown in Fig. 5a and are associated

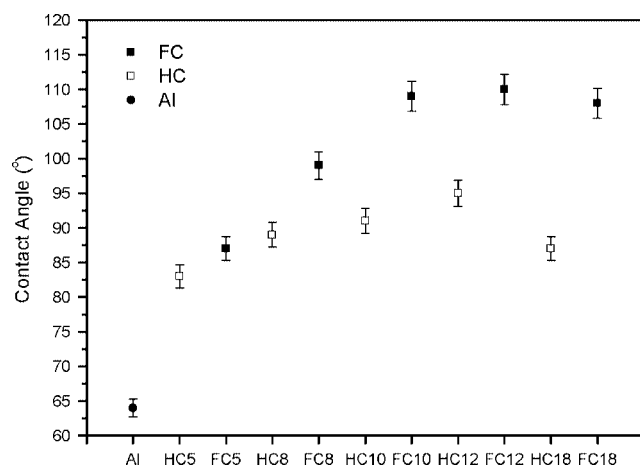


Figure 3. Measurement of contact angles for water on Al surface, perfluorinated carboxylic acid (FC) SAMs and hydrogenated carboxylic acid (HC) SAMs.

Table 1. Thicknesses of perfluorinated carboxylic acid and hydrogenated carboxylic acid SAMs on Al substrate

SAMs	Chain length	Thickness (Å)
Perfluorinated carboxylic acid	C5	19.5
	C8	23.8
	C10	25.2
	C12	26.5
	C18	30.7
Hydrogenated carboxylic acid	C5	20.1
	C8	22.9
	C10	24.2
	C12	24.7
	C18	25.8

with Al_2O_3 or $\text{AlO}(\text{OH})$ (74.7 eV) and Al (72.7 eV). This result indicates that the outmost layer of Al is converted into aluminum oxide under ambient condition. A single F1s feature resulting from FC18 adsorption on aluminum oxide is shown in Fig. 5b. The F1s feature at 688.7 eV is assigned to $-\text{CF}_2-$ and $-\text{CF}_3$ groups, which indicates the fluorine element on the substrate surface. Figure 5c displays the C1s spectra obtained from one set of FC SAMs with various chain lengths (C5–C18) on aluminum oxide surface. The C1s features are assigned to $-\text{CF}_3$ group (~ 293.5 eV), $-\text{CF}_2-$ group (C5: 292.1 eV to C18: 291.5 eV),^[21,33] carboxylate group (COO^- , 289.2 eV),^[34] and a feature (284.8 eV) associated with adventitious carbon possibly from airborne hydrocarbon contamination. It is suggested that the samples were strongly bonded with airborne organics (fatty acid, etc.), which were adsorbed at film defects and imperfections and were not easily removed by vacuum pumping. Similar phenomena have been reported in a previous study.^[21] It is also observed that the intensity of adventitious carbon decreased rapidly with increase of fluorocarbon chain length while that of COO^- and $-\text{CF}_3$ remained constant. This is because the long chain FC SAMs were densely packed and with fewer defects, which prevented airborne organics from adsorbing onto the film.

Figure 5d shows a similar tendency of increase in C concentration associated with the increase of chain length in HC SAMs. In addition, two features arose from C1s, as shown in Fig. 5d, the left

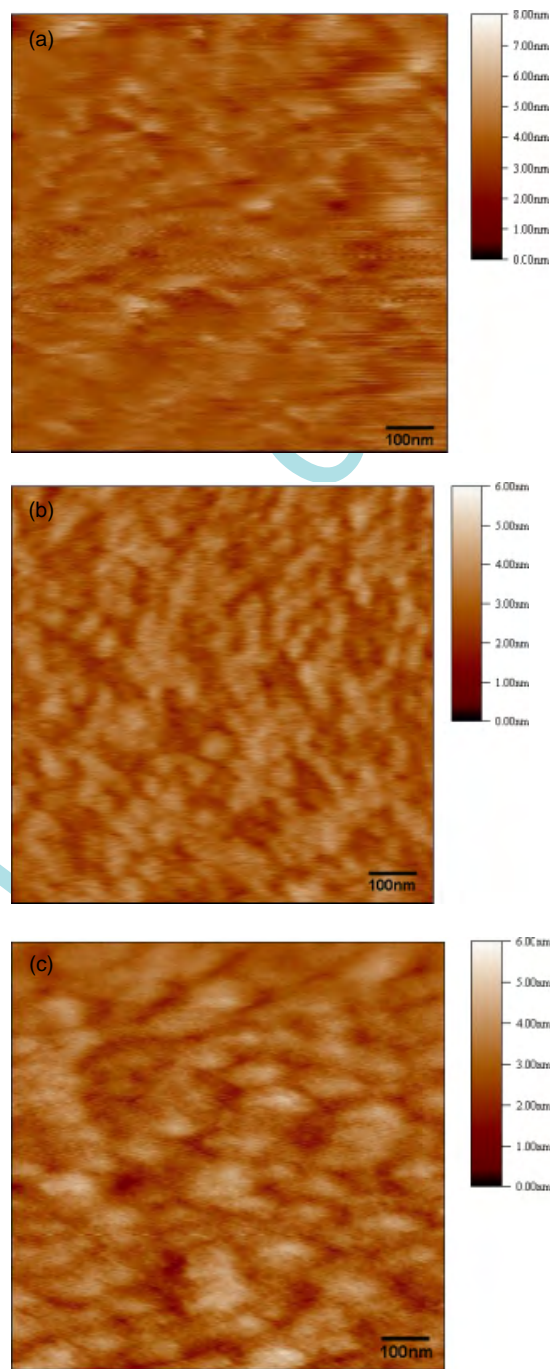


Figure 4. AFM morphologies of bare Al (a), FC12 SAMs (b) and HC12 SAMs (c). This figure is available in colour online at www.interscience.wiley.com/journal/sia.

feature assigned to carboxylate group (COO^- , 289.2 eV) and the right feature can be attributed to CH_x (284.8 eV).^[32]

Nanotribological behavior

AFM adhesion measurement under ambient condition

The adhesive force between AFM tip and SAM surfaces under various relative humidities are shown in Fig. 6. The bare aluminum surface showed higher adhesive force than SAMs deposited on it. Between FC and HC SAMs, the FC SAMs showed lower adhesion

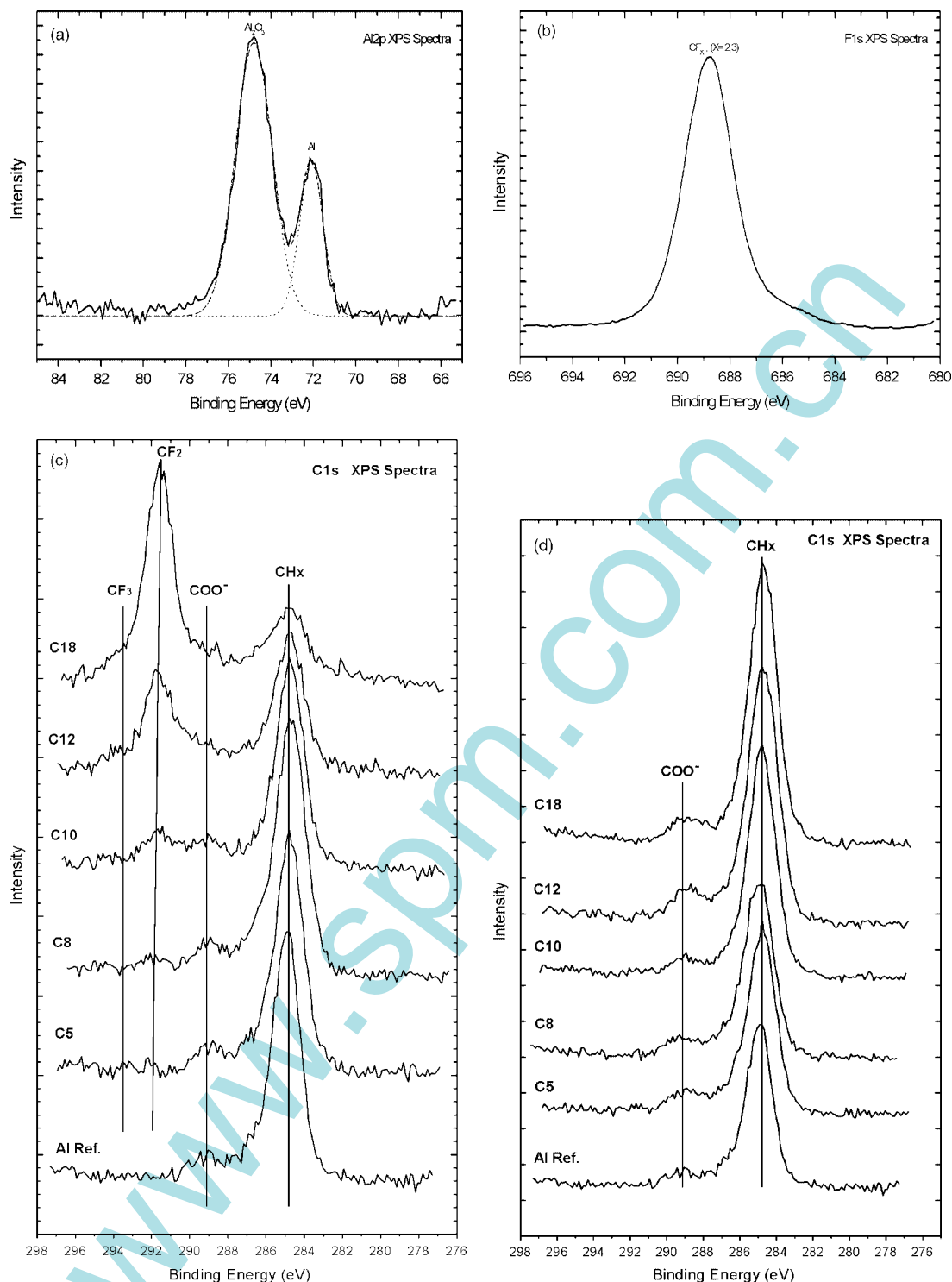


Figure 5. XPS spectra of Al 2p (a), F 1s (b), C 1s (c) region of the FC5-FC18 SAMs. (d) C 1s region of the HC5-HC18 SAMs.

force than HC SAMs with same chain length, which indicates that adhesive force is consistent with the difference in surface energy (15 mJ/m^2 for CF_3 -terminated compared to 19 mJ/m^2 for CH_3 -terminated SAMs^[35]). The relationship between adhesive forces for bare Al and FC SAMs with various chain lengths is shown in Fig. 6a. It shows that adhesive force increased with RH, which is due to water menisci contribution. It is also observed that the adhesive force of FC SAMs with chain lengths up to ten

carbons increased indistinctively and tended to a stable value. This tendency of the adhesive force agrees well with the change in contact angles (Fig. 3) which correlates with surface energy. FC12 and FC18 SAMs showed lowest adhesive forces and highest contact angles, which implies 12-carbon and 18-carbon chains are prone to form more stiff film. This is consistent with XPS measurement. As shown in Fig. 6b, a similar trend is observed for HC SAMs. In the case of short chain SAMs (n -carbon < 10), they

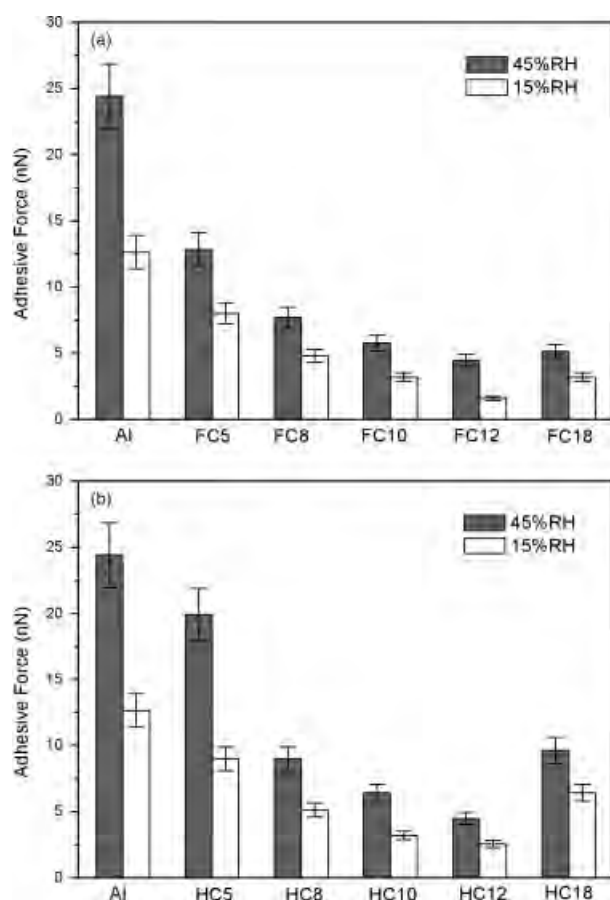


Figure 6. Relative humidity dependence of adhesion for Al substrate and various SAMs. (a) FC SAMs. (b) HC SAMs.

formed relatively soft monolayers and tended to disorder under the pressure applied by AFM tip. The pressure induced terminal defects may be sufficient for complete disorder, an effect that will be magnified by the reduced packing density of the short molecules.^[36] For SAMs with chain lengths up to ten carbons, low adhesive force may be attributed to high stiffness, which gives rise to a smaller contact area for the same applied load. Figure 7 shows the influence of temperature on adhesion. The adhesive force decreased with increase of temperature and then tended to a stable value. The drop in adhesive force is a result of desorption of water molecules and the corresponding decrease of water menisci contribution. The aluminum substrate and short chain SAMs showed more temperature dependence compared with long chain SAMs. The FC and HC SAMs with long chains exhibit temperature independence over the temperature range studied, which is due to the fact that highly hydrophobic nature of these monolayers results in less formation of water menisci. It indicates that long backbone chains and neighboring fluorine atoms provide stronger inter-chain interaction compared to that provided by short backbone chain and hydrogen atoms. SAMs with perfluorinated long chains were densely packed and highly ordered with solid-state-like properties at high temperature due to strong inter-chain Van der Waals force.

AFM nanofriction measurements

Figure 8 shows the relationship between friction force and external load for bare Al, as well as for FC and HC SAMs with various

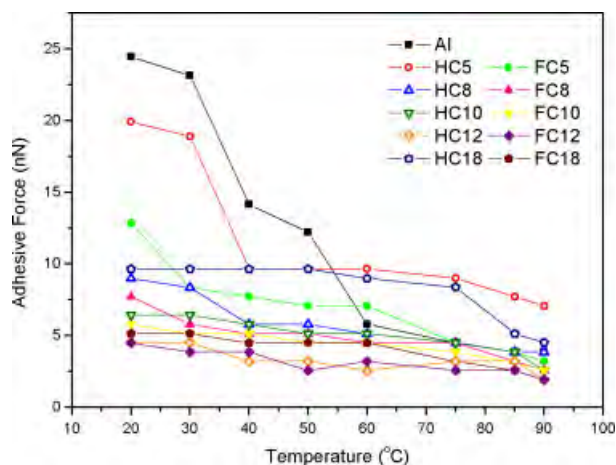


Figure 7. Dependence on temperature of adhesion for the Al substrate, FC SAMs (solid symbols) and HC SAMs (empty symbols). This figure is available in colour online at www.interscience.wiley.com/journal/sia.

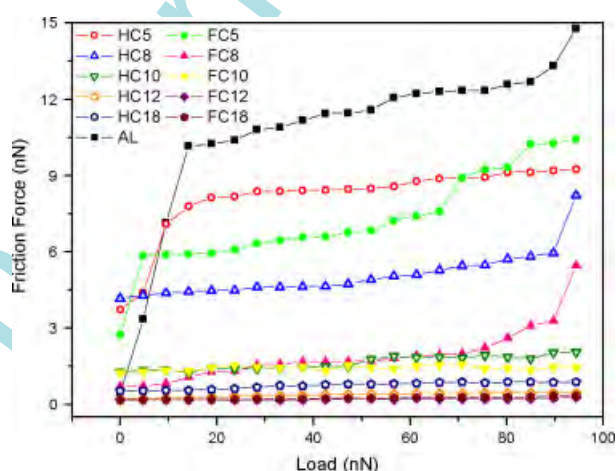


Figure 8. Plots of Friction force versus load for various SAMs on Al substrate, FC SAMs (solid symbols) and HC SAMs (empty symbols). This figure is available in colour online at www.interscience.wiley.com/journal/sia.

chain lengths, at RH of 15% and temperature of 20 °C. The bare aluminum surface without organic film generates the highest friction. This may be attributed to the highest surface energy on the Al_2O_3 -cover surface. The highest surface energy can be indicated by the lowest contact angle. It is a general tendency that the friction force decreases as chain length increases and FC SAMs showed lower friction force than HC SAMs of corresponding chain length. It is also observed that the friction properties of SAMs do not depend only on the chemical nature of terminal groups. Otherwise, all chain lengths should yield similar friction values. For the formation of SAMs, both surface energy and interchain interactions play important roles and determine quality and character of the SAMs.^[37] The decrease of friction is mainly due to SAMs with longer chain, as they generally possess relatively stronger inter-chain interaction, which give rise to a smaller contact area for the same applied load during the sliding.

Microtribological behavior

Figure 9 displays a function of friction force and external load for FC and HC SAMs. The data of microfriction show a similar tendency,

Table 2. Summary of tribological properties for the FC and HC SAMs on Al surface

SAMs property		Adhesive force	Nanofriction	Microfriction
Backbone style	Fluorocarbon backbone	Low	Low	High
	Hydrocarbon backbone	High	High	Low
Chain length	Short ($C_n < 10$)	High	High	–
	Middle ($C_n = 10–12$)	Low	Low	–
	Long ($C_n > 12$)	Low	Low	–
Terminal group	Methyl	High	High	Low
	Perfluorinated methyl	Low	Low	High

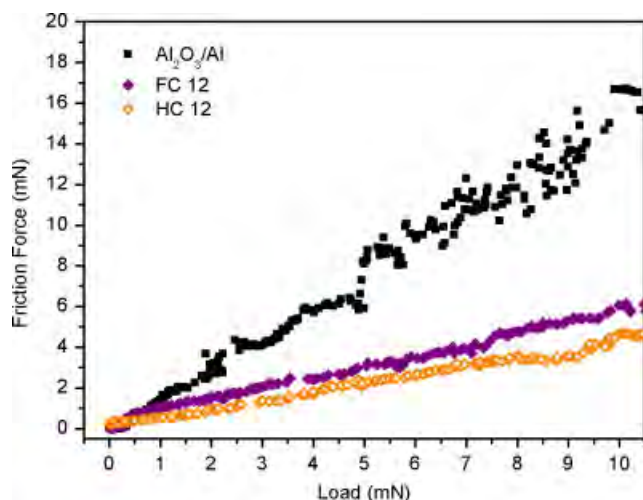


Figure 9. Microfriction behavior of Al substrate, FC12 and HC12 SAMs on sliding of a steel ball. (15%RH, 20 °C, velocity of 0.2 mm/s). This figure is available in colour online at www.interscience.wiley.com/journal/sia.

that is, the friction force increased with increasing external linear loads compared with the case of nanofriction (Fig. 8). However, an obvious discrepancy between the nano- and microfriction data is shown in Figs 8 and 9. The FC12 SAM exhibited lower friction force in nanoscale and it showed higher friction force in microscale compared to the HC12 SAM. It implies that the underlying mechanism may not be the same as friction in nanometer scale. This difference might be attributed to the higher stiffness of FC SAMs. For the fluorocarbon backbone chain, it is harder to rotate the backbone structure because of the much larger size of the fluorine atoms compared to that of the hydrogen atoms.^[38] On the other hand, the SAMs with hydrocarbon backbone chain possess more compliant backbone structure which may need less energy to be elastically deformed and in other energy dissipating modes during sliding.

Conclusions

Two series of perfluorinated carboxylic acid and hydrogenated carboxylic acid thin films were successfully assembled onto Al substrate by CVD. A comparative study is presented for the micro/nanoscale friction and adhesive properties of various SAMs with different hydrocarbon backbone chain and fluorocarbon backbone chain carboxylic acids assembled onto Al substrate. The influence of RH and temperature was investigated and the corresponding friction mechanisms were discussed. The

micro- and nanotribological characterization studies of the SAMs deposited on Al can be summarized as shown in Table 2. Compared with the results presented in other reports on fluorinated polymers, alkanethiolate, silane and alkylphosphonate,^[23,39–42] a similar tendency was shown, that is, the friction force reduced as chain length increased and fluorinated SAMs showed lower friction force than hydrogenated SAMs of corresponding chain length. Both of FC and HC SAMs deposited on Al substrate exhibited adhesion resistance and friction reduction. Long chain SAMs showed less dependence of adhesion on various RHs and temperatures than short chain SAMs. Furthermore, long chain FC SAMs exhibited an adhesion-resistance at various RHs and temperatures. FC SAMs exhibited better adhesion-resistance and nanofriction reduction than the corresponding HC SAMs. However, FC SAMs showed higher friction compared with HC SAMs in microscale. Thus, from a tribological point of view, the SAMs with compliant and long backbone chains and with terminal groups of low surface energy are intended for applications in lubrication and protection of MEMS/NEMS on aluminum-coated substrates.

Acknowledgements

This work was funded by National Natural Science Foundation of China (NSFC) under Grant Number 50675217 and National 973 Program under 2007CB607601.

References

- [1] S. M. Spearing, *Acta Mater.* **2000**, *48*, 179.
- [2] B. Bhushan, A. V. Kulkarni, M. Boehm, V. N. Koinkar, L. Odoni, C. Martelet, M. Belin, *Langmuir* **1995**, *11*, 3189.
- [3] R. Cucchiara, Multimedia surveillance systems, *Proc of the ACM VSSN*, ACM Press: New York, **2005**, p 1.
- [4] A. Ulman, *Chem. Rev.* **1996**, *96*, 1533.
- [5] E. Ostuni, L. Yan, G. M. Whitesides, *Colloids Surf., B* **1999**, *15*, 3.
- [6] A. Gulino, P. Mineo, E. Scamporrino, D. Vitalini, I. Fragala, *Chem. Mater.* **2004**, *16*, 1838.
- [7] J. Foisner, A. Glaser, T. Leitner, H. Hoffmann, G. Friedbacher, *Langmuir* **2004**, *20*, 2701.
- [8] M. Wang, K. M. Liechti, Q. Wang, J. M. White, *Langmuir* **2005**, *21*, 1848.
- [9] D. C. Bain, J. Evall, G. M. Whitesides, *J. Am. Chem. Soc.* **1989**, *111*, 7155.
- [10] G. N. Ralph, H. D. Lawrence, L. A. David, *J. Am. Chem. Soc.* **1990**, *112*, 558.
- [11] E. L. Paul, G. N. Ralph, G. M. Whitesides, *J. Phys. Chem.* **1992**, *96*, 5097.
- [12] R. S. Clegg, J. E. Hutchison, *Langmuir* **1996**, *12*, 5239.
- [13] R. C. Sabapathy, S. Shattacharyya, M. C. Leavy, W. E. Cleland, C. L. Hussey, *Langmuir* **1998**, *14*, 124.
- [14] O. Gershewitz, M. Grinstein, C. N. Sukenik, *J. Phys. Chem. B.* **2004**, *108*, 664.
- [15] S. Monsathaporn, F. Effenberger, *Langmuir* **2004**, *20*, 10375.

- [16] H. Liu, I. U. Ahmed, M. Scherge, *Thin Solid Films* **2001**, *381*, 135.
- [17] I. Touzov, C. B. Gorman, *J. Phys. Chem. B* **1997**, *101*, 5263.
- [18] K. H. Cha, D. E. Kim, *Wear* **2001**, *251*, 1169.
- [19] S. C. Clear, P. F. Nealey, *Langmuir* **2001**, *17*, 720.
- [20] S. Gauthier, J. P. Aime, T. Bouhacina, A. J. Attias, B. Desbat, *Langmuir* **1996**, *12*, 5126.
- [21] D. A. Hutt, G. J. Leggett, *Langmuir* **1997**, *13*, 2740.
- [22] D. A. Hook, S. J. Timpe, M. T. Dugger, J. Krim, *J. Appl. Phys.* **2008**, *104*, 034303.
- [23] B. Bhushan, M. Cichomski, E. Hoque, J. A. Derose, P. Hoffmann, H. J. Mathieu, *Microsyst. Technol.* **2006**, *12*, 588.
- [24] A. Ulman, *An Introduction to Ultrathin Organic Films: From Langmuir-Blodgett to Self-assembly*, Academic: San Diego, CA, **1991**.
- [25] S. L. Ren, S. R. Yang, Y. P. Zhao, T. X. Yu, X. D. Xiao, *Surf. Sci.* **2003**, *546*, 64.
- [26] X. D. Xiao, L. M. Qian, *Langmuir* **2000**, *16*, 8153.
- [27] V. V. Tsukruk, V. N. Bliznyuk, *Langmuir* **1998**, *14*, 446.
- [28] Y. H. Liu, T. Wu, D. F. Evans, *Langmuir* **1994**, *10*, 2241.
- [29] S. M. Hsu, P. M. McGuiggan, J. Zhang, Y. Wang, F. Yin, Y. P. Yeh, R. S. Gates, Scaling issues in the measurement of monolayer films, *NATO/ASI Proceedings on the Fundamentals of Tribology and Bridging the Gap between Macro- and Micro/Nanoscales, Nano Science Series: II, Mathematics, Physics and Chemistry*, vol. 10, Kluwer: Amsterdam, **2001**.
- [30] X. H. Zhang, R. S. Gates, S. Anders, S. M. Hsu, *Tribol. Lett.* **2001**, *11*, 15.
- [31] S. M. Hsu, *Tribol. Int.* **2004**, *37*, 537.
- [32] H. I. Kim, T. Koini, T. R. Lee, S. S. Perry, *Langmuir* **1997**, *13*, 7192.
- [33] R. Wallace, P. Chen, S. Henck, D. Webb, *J. Vac. Sci. Technol., A* **1995**, *13*, 1345.
- [34] J. J. Chance, W. C. Purdy, *Langmuir* **1997**, *13*, 4487.
- [35] Y. F. Miura, M. Takenaga, T. Koini, M. Graupe, N. Garg, R. L. Graham, T. R. Lee, *Langmuir* **1998**, *14*, 5821.
- [36] A. Lio, D. H. Charych, M. Salmeron, *J. Phys. Chem. B* **1997**, *101*, 3800.
- [37] X. D. Xiao, J. Hu, D. H. Charych, M. Salmeron, *Langmuir* **1996**, *12*, 235.
- [38] C. Chidsey, D. Loiacono, *Langmuir* **1990**, *6*, 682.
- [39] K. K. Lee, B. Bhushan, D. Hansford, *J. Vac. Sci. Technol., A* **2005**, *23*, 804.
- [40] M. Mcdermott, J. Green, M. Porter, *Langmuir* **1997**, *13*, 2504.
- [41] X. Xiao, J. Hu, D. Charych, M. Salmeron, *Langmuir* **1996**, *12*, 235.
- [42] T. Kasai, B. Bhushan, *J. Vac. Sci. Technol., B* **2005**, *23*, 995.

www.spm.com